

VENTILATION SYSTEM PERFORMANCE

11th AIVC Conference, Belgirate, Italy  
18-21 September 1990

Paper 17

CALCULATION OF THE AIR FLOW PATTERN  
IN A PROPOSED NEW EUROPEAN  
TEST CHAMBER FOR RADIATORS

A. Huber, A. Moser, Q. Chen

ETH Zürich  
Institut für Energietechnik - LES  
CH-8092 Zürich, Switzerland



## **Calculation of the air flow pattern in a proposed new European test chamber for radiators**

A. Huber, A. Moser and Q. Chen  
Swiss Federal Institute of Technology, Zürich  
Energy Systems Laboratory

A new European norm for measuring the heat transfer rate of radiators is under discussion [ CEN TC 130 ]. This testing can be done either in a closed chamber with cooled walls or in an open chamber with a controlled air supply.

The air flow pattern around a typical radiator is calculated for both types of chambers.

The calculation is done with the program PHOENICS, a finite volume program that solves the conservation equations for mass, momentum and energy. For turbulence, the  $k-\epsilon$  model is used with the Lam-Bremhorst correction for low Reynolds numbers.

It has been found that the flow field around the radiator looks the same for both types of chamber. In the closed chamber there is a recirculating zone at the ceiling. This can be avoided in the open chamber when the air change rate exceeds some minimum value. This minimum value for the air change rate is dependent only on the heat output of the radiator.

# BERECHNUNG DER STRÖMUNGSFELDER AM GEPLANTEN NEUEN HEIZKÖRPERPRÜFSTAND DER EMPA

## Zusammenfassung

Im Rahmen der EG-92-Normbestrebungen soll für die Heizkörperprüfung in Europa eine einheitliche Lösung gefunden werden. (CEN TC 130). Heute in Gebrauch sind einerseits die geschlossenen Prüfkammern, bei denen die Wärmeabfuhr durch die gekühlten Wände erfolgt und andererseits die offenen Prüfkammern (DIN 4704 und ISO TC 116). Als Entscheidungsgrundlage für die Typenwahl des neuen Prüfstandes sollten folgende Fragen beantwortet werden:

- Inwiefern beeinflusst bei einer offenen Prüfkammer ein Lufteinlass das Strömungsbild um den Heizkörper?
- Wie sieht bei einem typischen Heizkörper die Temperaturverteilung in einer geschlossenen und wie in einer offenen Kammer aus?
- Welche Temperaturen und Massenströme sind bei einem offenen Kammertyp am Lufteinlass zu wählen, und wie verändert eine Variation dieser Werte das Strömungsbild im Raum?

Zur Klärung dieser Fragen wurde am Laboratorium für Energiesysteme an der ETH Zürich eine rechnerische Variantenstudie sowohl am geschlossenen als auch am offenen Prüfkammertyp durchgeführt. Ausgeführt sind die Berechnungen mit PHOENICS, einem finite Volumen Programm, das die Impuls-, Kontinuitäts- und Energiegleichungen löst. Die Turbulenz wird mit dem  $k-\epsilon$  - Turbulenzmodell mit den Low-Reynolds-Erweiterungen nach Lam - Bremhorst bestimmt. (cf [2] - [18])  
Als Resultat der Untersuchungen können folgende Punkte festgehalten werden:

- Das Strömungsbild beim Heizkörper ist praktisch unabhängig vom Prüfkammertyp und Volumenstrom am Lufteinlass.
- In einer geschlossenen Prüfkammer gibt es an der Decke eine Rezirkulationszone.
- In einer offenen Prüfkammer tritt die Rezirkulation nur dann auf, wenn der Volumenstrom beim Heizkörper grösser ist als der Volumenstrom des Einlasses. Der minimale Volumenstrom am Einlass wird also durch die konvektive Wärmeleistung des Heizkörpers bestimmt.
- Rezirkulation ändert schlagartig das Strömungs- und Temperaturbild und kann die Regelung erschweren.

Die Änderung der konvektiven Wärmeleistung eines Heizkörpers bei verschiedenen Kammertypen kann wegen der getroffenen vereinfachenden Annahmen nicht beziffert werden.

## 1. Today's measurement of the heat transfer rate of radiators

The measurement of the heat transfer rate is described in the norms DIN 4704 and ISO TC 116. Open test chambers are allowed as well as closed ones. The test results of these two types of chamber are in any case not comparable. In Switzerland the closed type of test chamber is used (Fig. 1). The walls are cooled with water (Hartmann [1]). In other countries, as for example in Italy, the closed type with air cooled walls is in use. The open type of test chamber can be found in Stuttgart at the laboratory of Prof. Bach (Fig. 2).

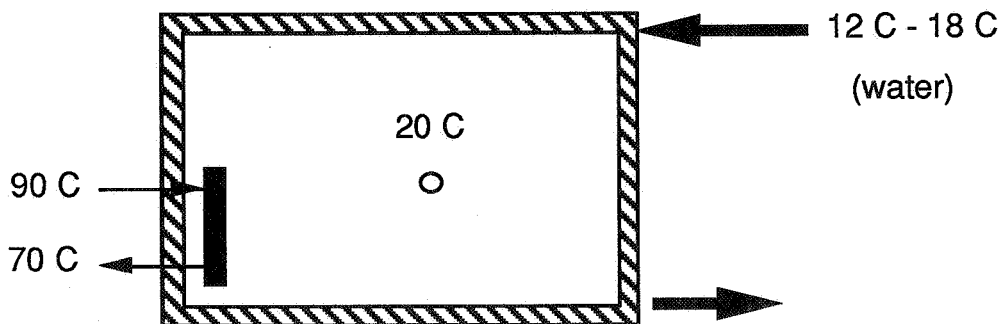


Fig. 1 : The closed type of test chamber at the EMPA, Switzerland

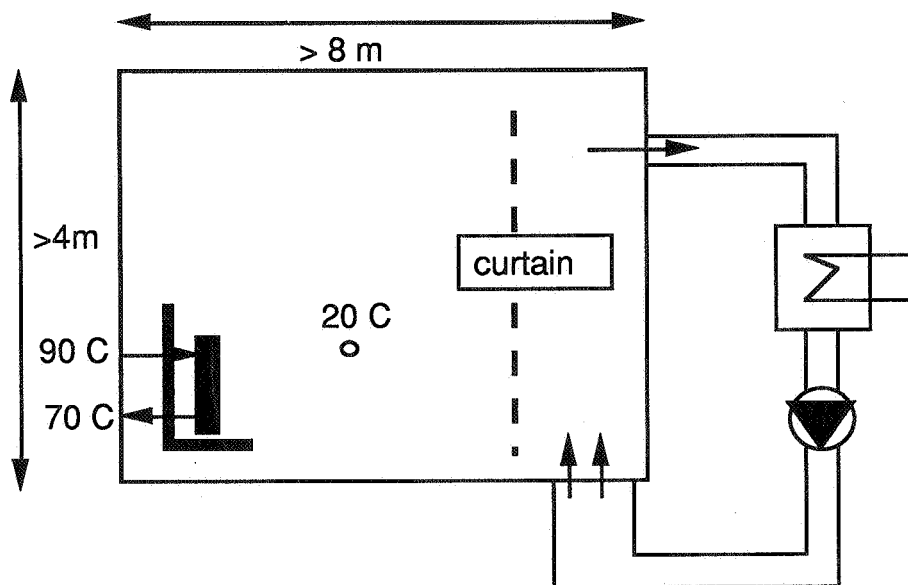


Fig. 2 : The open type of test chamber (DIN - norm)

An important disadvantage of a closed test chamber is the large time that is needed for measuring the heat transfer rate at different water temperatures in the radiator, since the chamber must be in equilibrium for each measurement. Another point is, that the walls of the different types of test chamber are at different temperatures and this leads to a different radiative heat transfer rate. This is one reason why the measurement of the same radiator in different test chambers can lead to different results. Another reason can be found in the different air flow patterns caused by these different wall temperatures.

## 2. Proposal of a new test chamber (CEN TC 130)

In the future in all European countries there will be only one type of radiator test chamber. This type will be described in a CEN norm (CEN TC 130). For this norm there is now an open as well as a closed type under discussion. For the closed type there is a water cooling system possible, or a system with air cooled walls ( Fig. 1 ). The open system would have water cooled walls that keep the walls at a constant temperature and an inlet with controlled air temperature and mass flow rate ( Fig. 3 ).

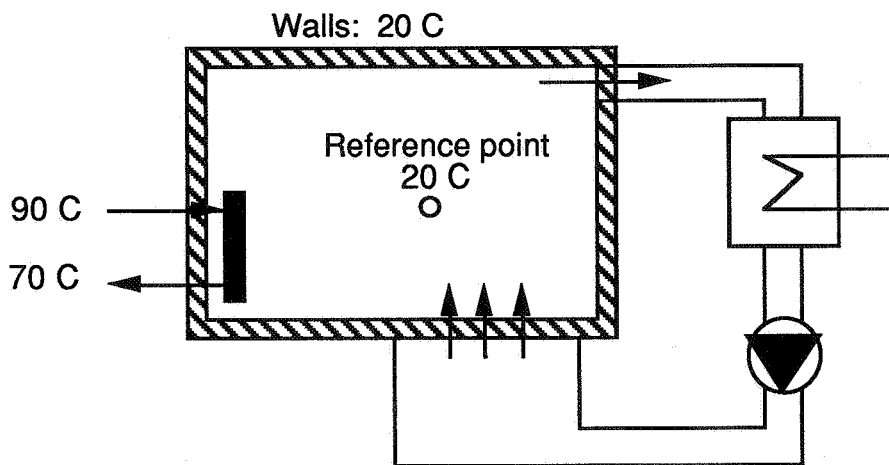


Fig. 3: Proposal of the new open type of test chamber

### 3. Geometry of the calculated two types of test chamber

The following pictures show the geometry of the two rooms for which calculations have been performed (Fig. 4 - 5 ). They do not have to correspond in every detail to the rooms that are discussed in TC 130. They only need to show us the principal differences in the air flow pattern and the temperature gradient in the two types of test chamber.

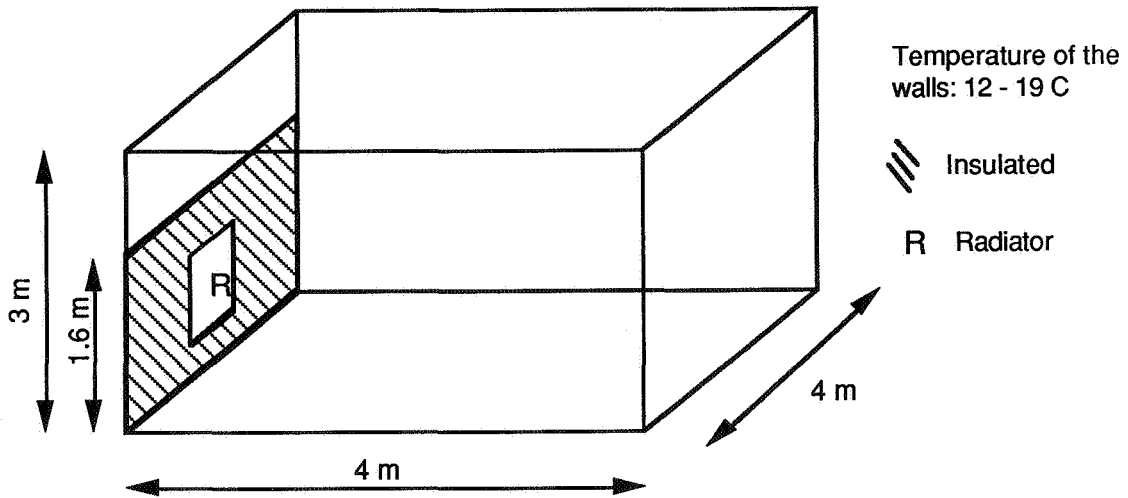


Fig. 4: Geometry of the closed test chamber

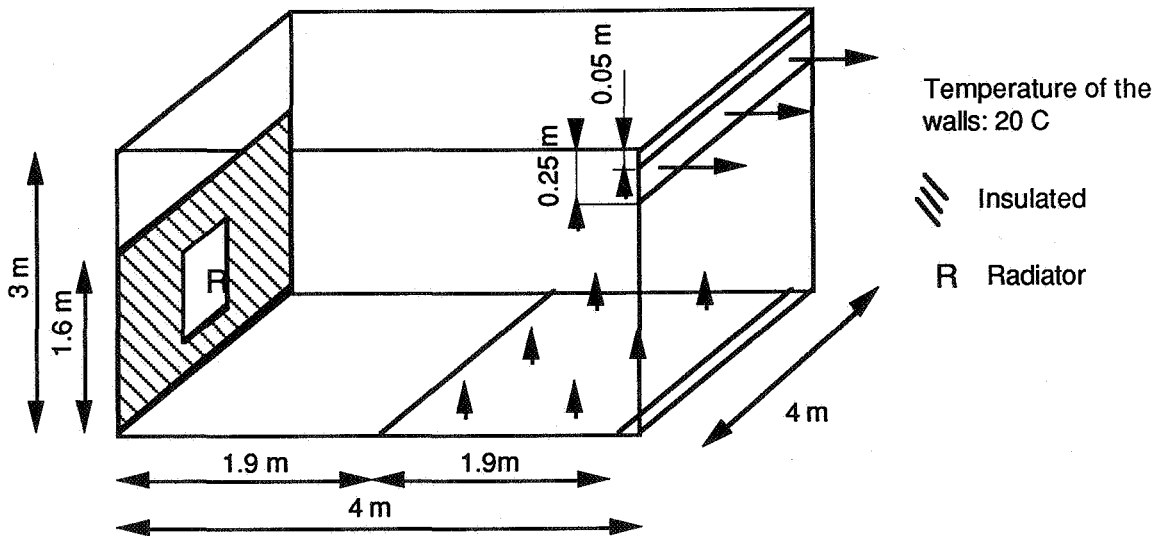


Fig. 5: Geometry of the open test chamber

#### 4. The Radiator

The calculation is based on a flat type of radiator as can be seen in Fig. 6:

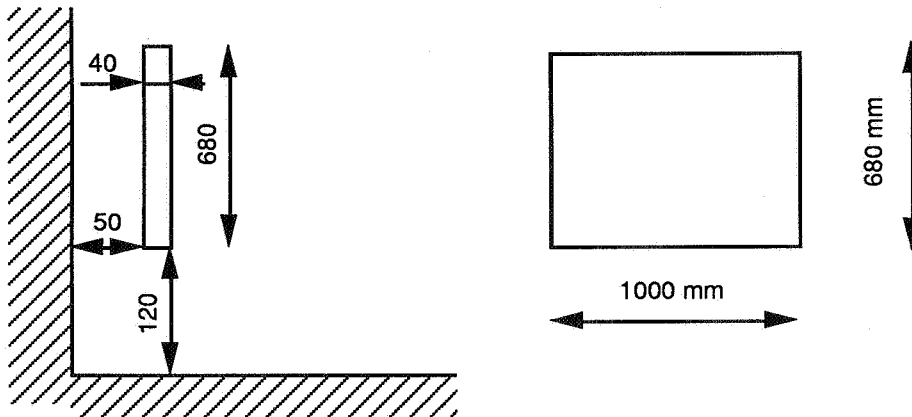


Fig. 6: Geometry of the radiator

From measurements of a similar type of radiator (Prolux, Typ S60) the following data have been found at the EMPA:

- heat transfer rate due to convection: 630 Watt
- heat transfer rate due to radiation: 420 Watt

In the calculation radiation can be neglected since the wall temperature is used as boundary condition and there is hardly any direct radiative heat transfer between the walls and the air.

There are two ways to model the radiator. The first is to model the temperature on the surface of the radiator. This can not be done without considering the mass flow in the radiator and the radiative heat transfer between the walls and the radiator. Neither of these is known at the start of the calculation, so the result can only be found in a iterative process. Once the surface temperature is known, the convective heat transfer can be calculated from the temperature gradient at the radiator, as is done at the other walls. Since it is not our goal to calculate the heat transfer rate of the radiator, and thus replace the measurement by a calculation, this method will no longer be looked at. What we actually want to know is the changing of the air flow pattern in different test chambers for a given convective heat transfer rate. Therefore the second possibility is chosen. Here a constant convective heat transfer rate is given as a source term. In our case it is 315 W on both sides of the radiator, so that we have a total convective heat transfer rate of 630 W.

## 5. Boundary conditions at the inlet for the open test chamber

Two different air change rates have been considered:

- 0.01 m/s inlet velocity, corresponding to a air change rate of 5.7 per hour
- 0.05 m/s inlet velocity, corresponding to a air change rate of 28.5 per hour.

When there is no recirculation from the ceiling an inlet temperature of 20 C is necessary to get a fixed temperature of 20 C at the reference point (Fig. 3). When there is recirculation, the inlet temperature must be lower since in this case the fresh air is mixed with the warm air from the ceiling. In the calculation the inlet temperature is always 20 C, so the temperature at the reference point is variable.

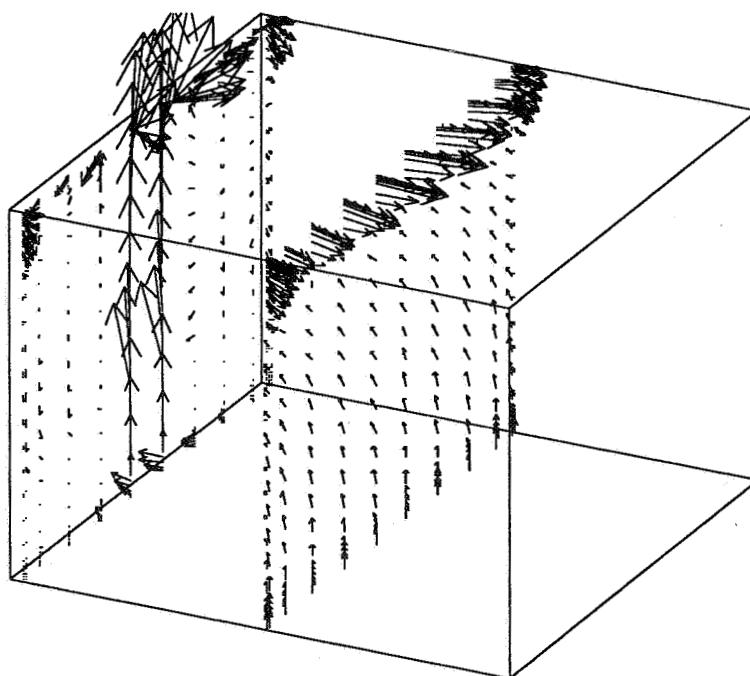


Fig. 7: Air flow pattern in the open test chamber,  
Run 88C: Velocity of the air at the inlet is 0.05 m/s

## 6. Wall temperatures in the closed test chamber

In the closed test chamber all energy must leave the room through the walls. Therefore the walls must be cooled to a temperature between 12C and 18C, depending on the heat transfer rate of the radiator.

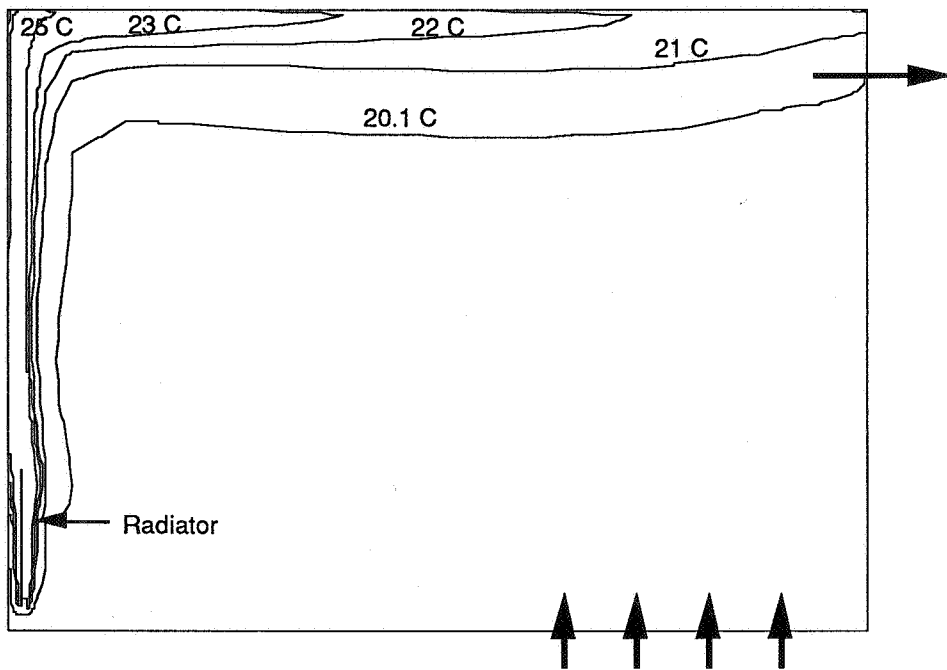
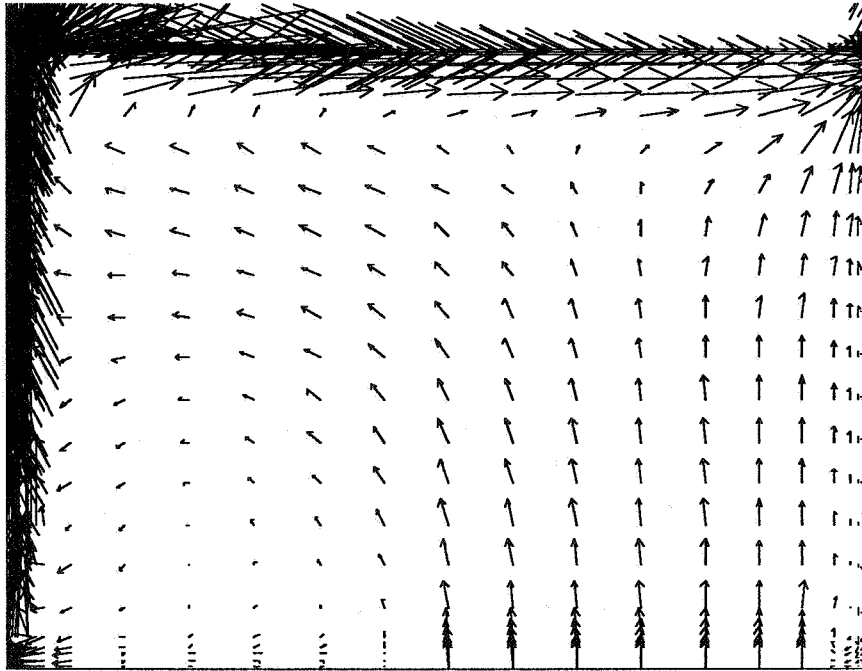
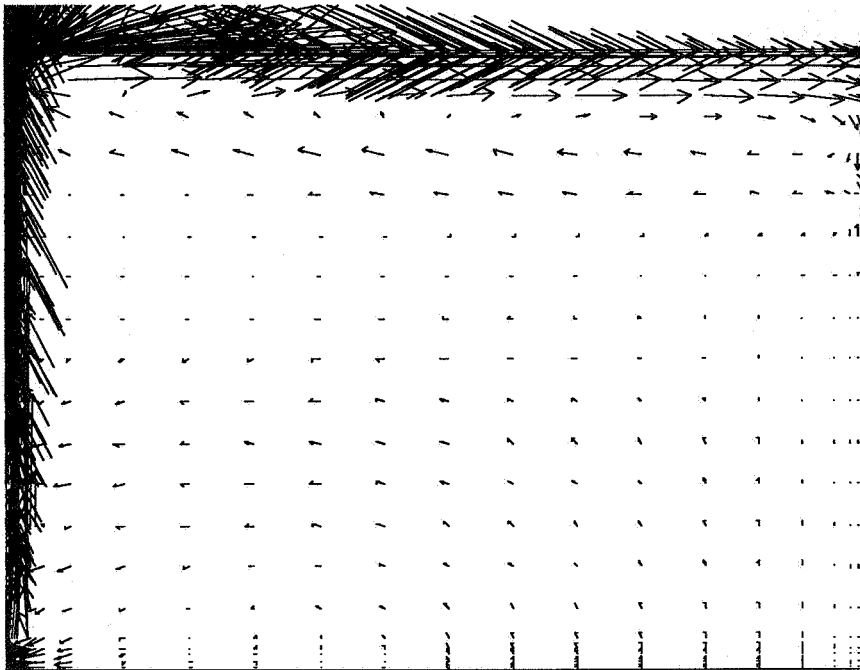


Fig. 8 - 9: Run 88C, open test chamber, air flow pattern and distribution of the temperature, inlet velocity: 0.05 m/s



→ 0.2 m/s

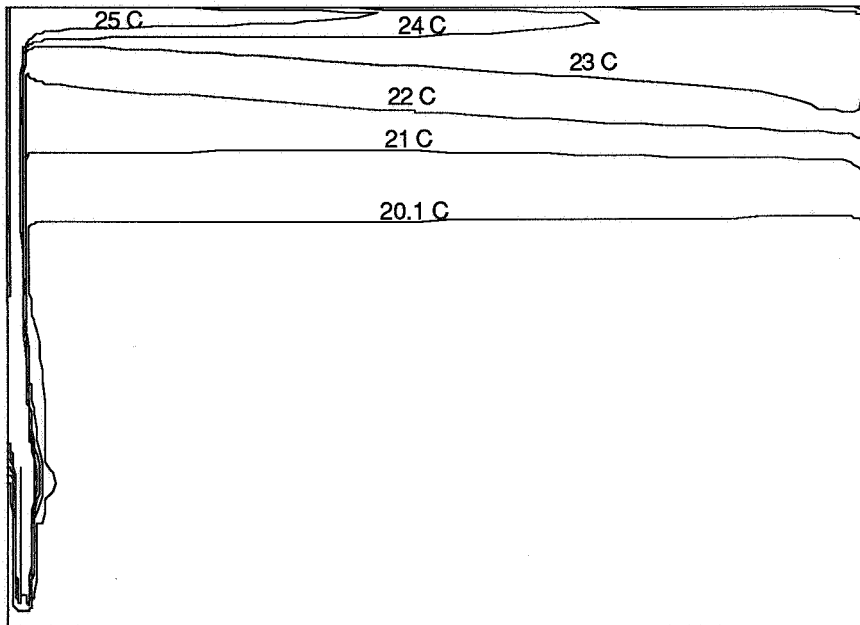
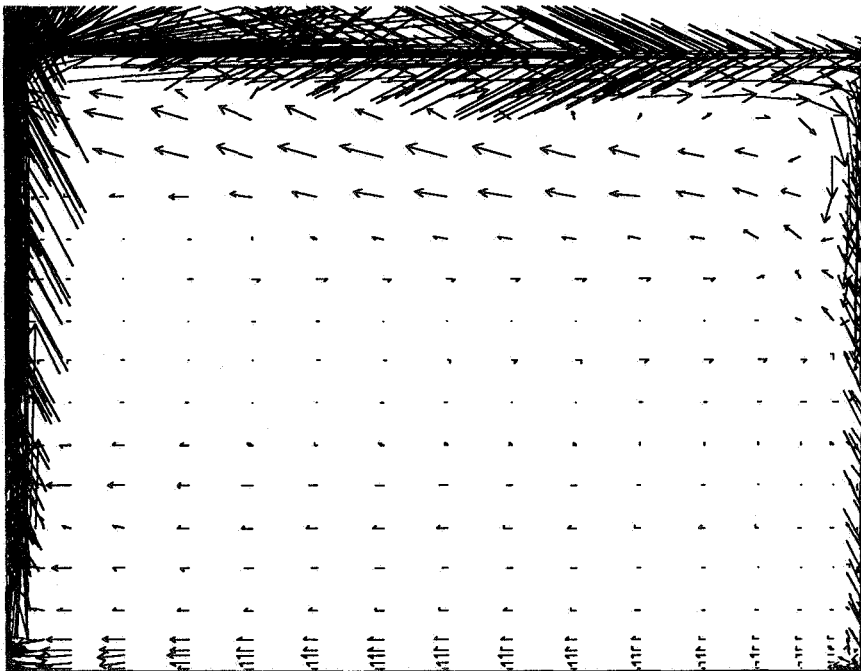
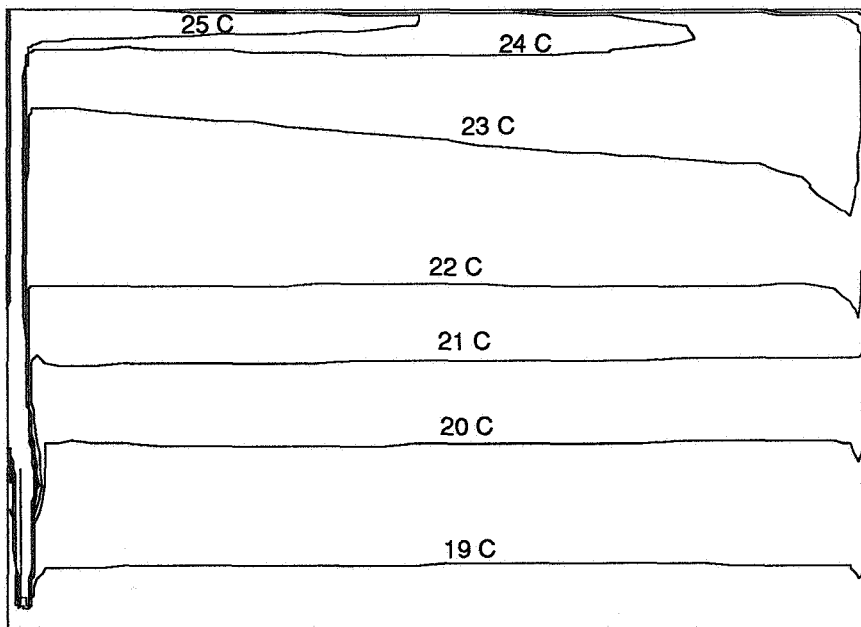


Fig. 10 - 11: Run 88E, open test chamber  
air flow pattern and distribution of the temperature,  
inlet velocity: 0.01 m/s



→ 0.2 m/s



**Fig. 12 - 13: Run 89C, closed test chamber  
air flow pattern and distribution of the temperature,  
wall temperature: 18 C**

## 7. The grid

Fig. 14 shows the grid for the calculation around the radiator. The first grid point is 0.5 mm away from the wall, the second 1.5 mm. The reason for this very fine grid can be found in the way the heat transfer at the walls is calculated. It is not calculated by any empirical Nusselt number formula but by calculating the temperature profile near the wall. This is possible because a low Reynolds number turbulence model is used. In total there are 42 x 31 x 20 grid points used in the calculation.

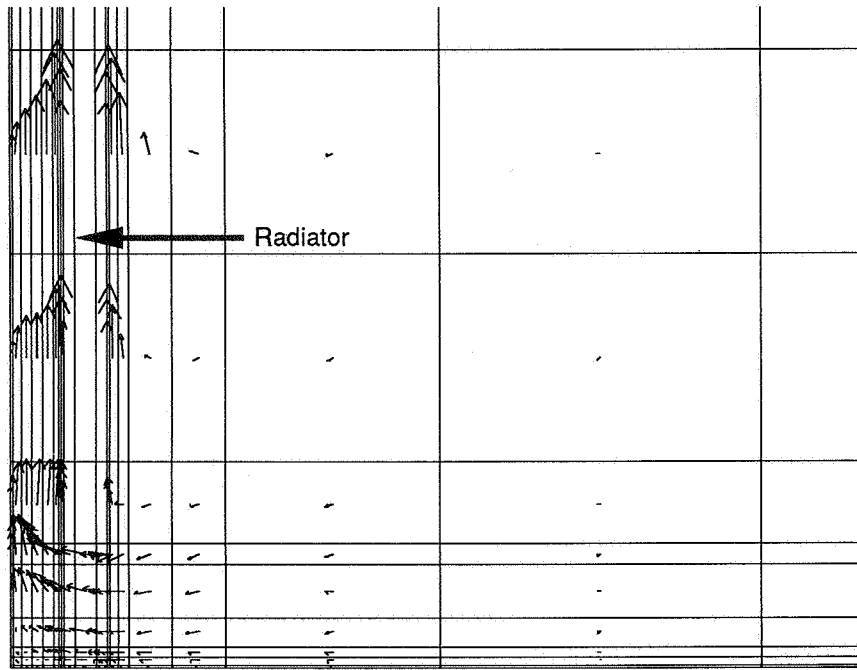


Fig 14: Grid around the radiator

## 8. The influence of the inlet velocity in the open test chamber

In order to investigate the influence of the inlet velocity on the air flow pattern and the temperature profile, the inlet velocity was reduced from 0.05 m/s (Fig. 8 - 9) to 0.01 m/s (Fig. 10 - 11) and a principal change in the air flow pattern can be seen. The mass flow of air at the radiator is about the same for both cases. The mass flow at the outlet must be the same as at the inlet. This means that when the mass flow of air at the radiator is greater than the mass flow at the inlet a recirculation is observed. To avoid this recirculation there is a minimum air change rate necessary that depends only on the convective heat transfer rate of the radiator.

Recirculation means that the hot air from the ceiling is mixed with the fresh air from the inlet. This could cause problems in controlling the temperature at the reference point and prolongs the measurement.

## 9. Outline of the mathematical models

Recent developments of numerical techniques to solve the basic equations of fluid mechanics and the advent of supercomputers have led to the opportunity to compute space air diffusion as reviewed by Nielsen [17] and Ceschi [18]. With these techniques, it is possible to study the field distributions of air velocity, temperature and turbulence intensity.

In the present study, the airflow program developed by Rosten and Spalding [14] has been employed to calculate air distribution. The computations involve the solution of three-dimensional equations for the conservation of mass, momentum ( $u, v, w$ ), energy ( $H$ ), turbulence energy ( $k$ ), and the dissipation rate of turbulence energy ( $\epsilon$ ). The turbulence model used is the low Reynolds number  $k-\epsilon$  model of Lam and Bremhorst [11] that has been implemented in the airflow program. This model has been verified to be more suitable for indoor airflow simulations, and a better agreement between computation and experiment has been found with respect to velocity and turbulence energy distributions and heat exchange through solid walls (Chen et al. [6]). The governing equations of the model can be expressed in a standard form:

$$\text{div} (\rho \vec{V} \Phi - \Gamma_{\Phi} \text{grad} \Phi) = S_{\Phi} \quad (1)$$

where  $\rho$  is the air density ( $\text{kg}/\text{m}^3$ ),  $\vec{V}$  is the air velocity vector ( $\text{m}/\text{s}$ ),  $\Gamma_{\Phi}$  is the diffusive coefficient ( $\text{kg}/\text{sm}$ ),  $S_{\Phi}$  is the source term of the general fluid property, and  $\Phi$  can be any one of  $1, u, v, w, k, \epsilon$  or  $H$ . When  $\Phi = 1$  the equation changes into the continuity equation.

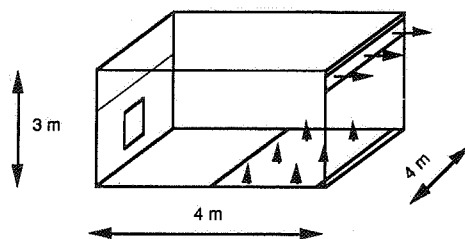
## 10. Conclusions

- It is possible to calculate the air flow pattern around a radiator with a known convective heat flux, and numerical simulation allows prediction of parameter sensitivity.
- The amount of computing time is huge (cf. appendix A).
- The air flow pattern around the radiator is independent of the type of test chamber (open or closed) and of the inlet velocity ( $0.01 \text{ m/s}$  or  $0.05 \text{ m/s}$ ).
- In a closed test chamber there is always a recirculation zone at the ceiling.
- In the closed test chamber a recirculation can be observed, when the inlet mass flow is smaller than the mass flow at the radiator. The mass flow at the radiator is only dependent on its convective heat output.
- Recirculation changes the air flow pattern and the temperature distribution in the room entirely.

## References

- 1) **P. Hartmann (1973):**  
Der Heizkörperprüfstand der EMPA.  
Schweizerische Blätter für Heizung und Lüftung, Heft Nr. 4/73
- 2) **D. Aiulfi (1986):**  
Numerische Berechnung eines Luftstrahls mit dem  $k - \epsilon$  - Turbulenzmodell, und Vergleich mit Messungen; Interner Bericht ETHZ-LES
- 3) **D. Aiulfi (1990):**  
Simplified Combustion Models for Turbulent Gas Diffusion Flames  
Diss. ETH Zürich
- 4) **J. Borth, K. Eisele (1988):**  
Vergleich von LDA - Messungen mit Ergebnissen der numerischen Simulation am Beispiel eines klimatisierten Raumes. Teil II : Numerik ; Interner Bericht Nr. 1704, Gebr.SULZER AG.
- 5) **Q. Chen (1988):**  
Indoor Airflow, Air Quality and Energy Consumption of Buildings.  
Ph.D. thesis, Delft University of Technology.
- 6) **Q. Chen, A. Moser, A. Huber (1990):**  
Prediction of Buoyant, Turbulent Flow by a Low-Reynolds-Number  $k-\epsilon$  Model.  
ASHRAE Transactions 1990, V.96, Pt.1.
- 7) **L. Davidson (1989):**  
Numerical Simulation of Turbulent Flow in Ventilated Rooms  
Ph.D. thesis, Chalmers University of Technology, Göteborg, Sweden
- 8) **H. Durrer (1988):**  
Numerische Ermittlung von Luftströmungen im Einzelraum. 2.Status-Seminar ERL  
Seite 43.
- 9) **A. Heiss (1987):**  
Numerische und experimentelle Untersuchungen der laminaren und turbulenten Konvektion in einem geschlossenen Behälter  
Diss. TU München
- 10) **A. Huber , A. Moser (1989):**  
Numerische Ermittlung von Luftströmungen im Einzelraum. 3.Status-Seminar ERL  
Seite 17.
- 11) **C. Lam, B. Bremhorst (1981):**  
A Modified Form of the  $k - \epsilon$  - Model for Predicting Wall Turbulence; Transactions of the ASME, Vol. 103
- 12) **P. Nielsen (1979):**  
Buoyancy-Affected Flows in Ventilated Rooms; Numerical Heat Transfer, Vol.2
- 13) **S. Patankar (1980):**  
Numerical Heat Transfer and Fluid Flow  
Hemisphere Publishing Corporation
- 14) **H. Rosten, B. Spalding (1987):**  
The Phoenix Reference Manual.  
Software Version 1.4, CHAM Report number TR200
- 15) **A. Schachenmann, D.Wiss, G.Metzen (1990):**  
Numerische Berechnung von Raumluftrömungen und Vergleich mit LDA-Messungen im Fall freier und erzwungener Konvektion  
Technische Rundschau SULZER, 1/1990, Seite 30.
- 16) **Chr. Schönenberger (1988):**  
Low Reynolds Number Turbulence Model; Interner Bericht ETHZ-LES
- 17) **P. Nielsen (1989):**  
Progress and trends in air infiltration and ventilation research,  
Proceedings of the 10th AIVC Conference
- 18) **P.A. Ceschi (1990):**  
Numerische Berechnung eines turbulenten ebenen Strahls.; Interner Bericht ETHZ-LES

## Short description of run 88C



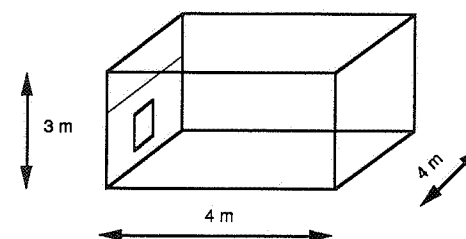
- Computing program:- PHOENICS of CHAM Ltd, London
- Algorithm: - Finite volume  
- SIMPLEST - algorithm  
- Upwind - interpolation  
- steady calculation
- grid: - 42 x 31 x 20  
- Staggered grid
- Turbulence model: - Low-Reynolds  $k - \epsilon$  model of Lam-Bremhorst [11]  
- Turbulent Prandtl number: 0.9
- Buoyancy: - With Boussinesq approximations
- Boundary conditions:- Convective heat transfer rate at the radiator: 630 W  
- Velocity at the walls 0 m/s  
- Linear / logarithmic wall formulae  
- Wall temperature: 20 C  
-  $k$  and  $\epsilon$  at the 1st grid point:

$$k = \frac{\tau_w}{\rho \sqrt{0.09}}$$

$$\epsilon = \frac{0.1643}{0.435} k^{1.5} \frac{1}{d}$$

- Inlet conditions - Velocity 0.05 m/s  
- Area 1.9 m x 4 m  
- Temperature 20 C  
-  $k$  0 m<sup>2</sup>/s<sup>2</sup>  
-  $\epsilon$  0 m<sup>2</sup>/s<sup>3</sup>
- CPU time: - 2500 sweeps, 10h CPU-time Cray-XMP

## Short description of run 89C



- Computing program:- PHOENICS of CHAM Ltd, London
- Algorithm: - Finite volume  
- SIMPLEST - algorithm  
- Upwind - interpolation  
- steady calculation
- grid: - 42 x 31 x 20  
- Staggered grid
- Turbulence model: - Low-Reynolds  $k - \epsilon$  model of Lam-Bremhorst [11]  
- Turbulent Prandtl number: 0.9
- Buoyancy: - With Boussinesq approximations
- Boundary conditions:- Convective heat transfer rate at the radiator: 630 W  
- Velocity at the walls 0 m/s  
- Linear / logarithmic wall formulae  
- Wall temperature: 18 C  
-  $k$  and  $\epsilon$  at the 1st grid point:

$$k = \frac{\tau_w}{\rho \sqrt{0.09}}$$

$$\epsilon = \frac{0.1643}{0.435} k^{1.5} \frac{1}{d}$$

- CPU time: - 2500 sweeps, 10h CPU-time Cray-XMP

Discussion

Paper 17

**M J Holmes (Arup R & D, UK)**

How did you handle radiant heat transfer in your simulation?

*A. Huber & A Moser (ETH, Zurich, Switzerland)*

*Earlier measurements have shown that the radiator heat output is about 60% convection and 40% radiation. In a typical case the 60% convection amounts to 630W. These 630W have been used as heat source at the radiator for the air flow simulation. Radiative exchanges between walls were not computed because the walls had a prescribed temperature of 20 degrees C.*